Available online at www.sciencedirect.com
SCIENCE DIRECT®
Thin Solid Films 450 (2004) 23–28
thin solid films
www.elsevier.com/locate/tsf

Recent advances in characterization of ultra-thin films using specular X-ray reflectivity technique

S. Banerjee[a,*], S. Ferrari[b], D. Chateigner[c], A. Gibaud[d]

[a]*Saha Institute of Nuclear Physics, 1/AF Bidhan Nagar, Calcutta 700 064, India*
[b]*Lab. MDM – INFM via Olivetti 2, 20041 Agrate Brianza, Milan, Italy*
[c]*CRISMAT-ISMRA, Caen, France*
[d]*Laboratoire de Physique de l'Etat Condens, UPRES A 6087 CNRS, Faculté des Sciences, Université du Maine, Le Mans, France*

Abstract

We will present different approaches to analyze the specular grazing incidence X-ray reflectivity (GIXR) data to characterize ultra-thin films. The analysis of the GIXR data yields structural parameters such as surface and interfacial roughness, density profiles and total thickness of the film and its individual layers if the film consists of many layers. We shall describe three schemes here (1) a model dependent method based on dynamical scattering, which is generally known as recursive formalism, (2) a model independent method based on distorted wave Born approximation and (3) an inversion technique based on Born approximation. We will point out the problem of the non-uniqueness of the solutions, which are generally encountered in analyzing the X-ray reflectivity data based on the recursive formalism when the experimental data are fitted using non-linear least square fitting technique to obtain the fit parameters. We will demonstrate the above formalisms on few systems as case studies. We will also show how to converge to a realistic solution combining the above mentioned formalisms.

PACS: 68.55.Jk; 61.10Kw

Keywords: X-ray reflectivity; Ultra-thin films; Surface and interfaces

1. Introduction

Structural characterization of ultra-thin films and multi-layers is technologically very important. Characterizations of these films are necessary to design the films with required physical properties. Grazing incidence X-ray reflectivity (GIXR) technique is becoming popular for structural characterization of ultra-thin inorganic and organic films. This is a non-destructive tool for structural characterization of ultra-thin films and multi-layer structures. In GIXR technique, the X-ray beam is incident on the sample at a grazing angle and the interfered reflected beam is collected by an X-ray counter. The interference occurs due to the presence of interfaces in the sample. The interference periods depend on the thickness of the layers and the amplitude of the interference oscillations depends on the contrast of the electron density between the layers and the interfacial roughness. Thus, the GIXR data contain structural information of the film such as thickness, densities and roughness of the film and its individual layers.

Various analysis schemes for X-ray reflectivity data are existing now but depending on the system to be studied one has to choose from the available schemes the one that can generate truthfully the parameters having real physical values and simultaneously generates the experimental reflectivity data accurately. There are now mainly three schemes to analyze the X-ray reflectivity for ultra-thin films and they are (1) a model-dependent scheme based on dynamical multiple scattering leading to a recursive formula [1–4], (2) model-independent method based on distorted wave Born approximation (DWBA) [5–9] and (3) a Fourier inversion technique based on Born approximation (BA) [10,11]. As a case study, we will demonstrate the above three formalisms on two ultra-thin film systems: (1) an ultra-thin film of TiN grown by chemical vapour depo-

*Corresponding author.

0040-6090/04/$ - see front matter © 2003 Elsevier B.V. All rights reserved.
doi:10.1016/j.tsf.2003.10.042

sition (CVD) technique and (2) an oxynitride ultra-thin film.

2. Analysis schemes for specular X-ray reflectivity

2.1. Recursive formalism

To analyze the X-ray reflectivity data, one generally uses a recursive formalism similar to Parratt's formalism [1] or the matrix method [2–4] to obtain the structural parameters of the film such as the thickness, the interfacial roughness and the electron density of the layers. In the above formalism the total film is considered to be consisting of $n+1$ layers and the X-ray reflectivity as a function of scattering wave vector k ($k=2\pi/\lambda$) is expressed by a recursive formula:

$$r_{n-1,n}(k)=\frac{r'_{n-1,n}+r'_{n,n+1}\exp(2id_nk_n)}{1+r'_{n-1,n}r'_{n,n+1}\exp(2id_nk_n)} \quad (1)$$

where $r'_{n-1,n}$ is Fresnel reflectance coefficient for the interface of layer n and layer $n-1$ and is equal to $(k_{n-1}-k_n)/(k_{n-1}+k_n)$. The label $n+1$ is for the substrate and $n=0$ is the label for the air. k_n is the scattering wave vector in the nth layer and $k_n=(k_0^2-k_{c,n}^2)^{1/2}$ where $k_0=(2\pi/\lambda)\sin\theta$ and $k_{c,n}=(2\pi/\lambda)\sin\theta_{c,n}$, θ and $\theta_{c,n}$ are the angle of incidence and critical angle for the total external reflection, respectively. Electron density of the layer is related to $\theta_{c,n}(\sim\lambda(r_e\rho_e/\pi)^{1/2})$, where λ is the incident wavelength of the X-ray beam, ρ_e is the electron density of the film and is related to mass density of the film [12] and r_e is the electron radius (2.8×10^{-5} Å). For specular reflectivity the angle of incidence is equal to the angle of reflection. The reflectance coefficient obtained at the detector is $r_{0,1}$. $r_{n-1,n}$ is used to calculate the reflectance for the layer above the substrate and recursively one can obtain $r_{0,1}$. To take into account the interfacial roughness, one has to multiply each of the reflectance coefficients by $\exp(-2k_n^2\sigma_n^2)$ [13], where σ_n is the interfacial roughness of the nth interface. We use the above expression Eq. (1) to fit the reflectivity data. In the recursive formalism one has to use a user-defined model for the structure of the film across its depth, which consists of a number of layers (boxes) describing the film. By fitting the reflectivity data using Eq. (1) one obtains the thickness d_n, electron density (obtained from $k_{c,n}$) and interfacial roughness (σ_n) as the fit parameters.

2.2. Distorted wave Born approximation formalism

This is a model independent scheme based on DWBA. This scheme works well for only ultra-thin films for thickness <400 Å having small variation in the density of the film across its depth. In this scheme the film is considered to be composed of number of thin virtual slices or boxes of electron density ρ_i of the ith slice/box. If one can evaluate the density of each box, then one obtains the density profile of the film as a function of depth. The reflectivity of the film using DWBA formalism is expressed as [5–9]:

$$R(k)=\left|ir_0(k)+\frac{(2\pi r_e)}{k}(a^2(k)\Delta\rho(q_z^f)+b^2(k)\Delta\rho^*(q_z^f))\right|^2 \quad (2)$$

The first term in Eq. (2) containing $r_0(k)$ is the specular reflectance coefficient of the film with an average electron density (AED) of ρ_0. The second term in Eq. (2) is for the small fluctuation of the electron density $\Delta\rho(z)$ over ρ_0 across the film where $a(k)$ and $b(k)$ are the transmission and reflection coefficient in the film, respectively, and r_e is the electron radius. $q_z=2k_z=4(\pi/\lambda)\sin\theta$, q_z^f $[=(q_z^2-q_c^f)^{1/2}]$ is the wave vector in the film, the subscript c indicates the critical value of the wave vector having a critical angle (θ_c) up to which the total external reflection occurs and the superscript f indicates the value of the wave vector in the film. The $\Delta\rho(q_z^f)$ is the Fourier transform of variation of electron density $\Delta\rho(z)=\rho(z)-\rho_0$, where z is the depth of the film and is expressed as

$$\Delta\rho(q_z^f)=\int_{-\infty}^{\infty}\Delta\rho(z)e^{iq_zf}dz \quad (3)$$

and $\Delta\rho(q_z^f)$ can be written in summation form in terms of $\Delta\rho_i$ $(=\rho_i-\rho_0)$ of thickness d of the ith box as

$$\Delta\rho(q_z^f)=\frac{i}{q_z^f}\left[\left(\sum_{j=2}^{j=N}(\Delta\rho_j-\Delta\rho_{j-1})e^{iq_z^f(j-1)d}+\Delta\rho_1-\Delta\rho_N e^{iq_z^fNd}\right)\right] \quad (4)$$

where N is the total number of boxes used in the calculation. By selecting the appropriate number of boxes and ρ_0 of the film, we fit Eq. (2) with $\Delta\rho_i$ as the fit parameters after convoluting the data with Gaussian instrumental resolution function. The initial value of $\Delta\rho_i$s is set equal to zero for the fitting.

2.3. Iterative scheme using Born approximation formalism

If we consider scattering wave vector greater than the critical value q_c, i.e. angle greater than θ_c the critical angle for total external reflection, then the X-ray reflec-

tivity can be expressed as the Fourier transformation of the derivative of the electron density profile (EDP) ($\rho'(z) = d\rho(z)/dz$) by [14,15]

$$R(q) = R_F(q)\left|\frac{1}{\rho_\infty}\int_{-\infty}^{\infty}\rho'(z)\exp(iqz)\right|^2 \quad (5)$$

where ρ_∞ and $R_F(q)$ are the electron density and Fresnel reflectivity of the substrate, respectively. From Eq. (5) we can easily obtain the auto-correlation function of the derivative of the density profile by taking Fourier transform of the ratio of reflectivity data and $R_F(q)$, i.e.

$$\mathrm{ACF}[\rho'(z)] = \int_{-\infty}^{\infty}\rho'(t)\rho'(t-z)dt$$

$$= \mathrm{const}\int_{-\infty}^{\infty}\frac{R(q)}{R_F(q)}\exp(-iqz)dz \quad (6)$$

The peaks in the Fourier spectrum indicate the layer thickness involved. In this scheme, one tries to obtain the actual EDP as a function of depth normal to the film from the initial guess model. The guess is made using the layer thickness of the film obtained from the Fourier spectrum and the AED value of the film from the value of q_c. From Eq. (5), one can obtain the reflectivity profile $R_m(q)$ from the derivative of the EDP of the model ($\rho'_m(z)$). The experimental data we denote by $R_e(q)$. By taking its ratio with $R_m(q)$, one can express the actual derivative of EDP ($\rho_e'(z)$) as [10,11]

$$\rho'_e(z) = F^{-1}\left[\sqrt{\frac{R_e(q)}{R_m(q)}}F[\rho'_m(z)]\right] \quad (7)$$

In the above expression F and F^{-1} are the forward and inverse Fourier transform pair. In analyzing the reflectivity data, an iterative procedure is carried out with Eq. (7) where we initially use a model profile $\rho_m(z)$ to generate a profile $R_m(q)$ and hence obtain the $\rho'_e(z)$. The model reflectivity profile $R_m(q)$ for the next iteration is now calculated by setting $\rho_m(z)$ equal to $\rho_e(z)\left[=\int dz\rho'_e(z)\right]$ of the previous iteration. Continuing the iteration, the model EDP will slowly converge to the actual EDP. It converges because the information regarding the actual experimental peak position of $\rho'_e(z)$ is contained in $F^{-1}[\sqrt{R_e(q)}]$, which is convoluted with two other functions $F^{-1}[1/\sqrt{R_m(q)}]$ and $\rho'_m(z)$. With successive iteration, $R_m(q)$ should tend towards $R_e(q)$ since $\rho_m(z)$ gets modified and the procedure should converge to the actual peak position of $\rho'_e(z)$, provided the model is within the radius of convergence of the experimental profile. In practice, the refinement of the density profile is obtained by selecting a window of the size of the film thickness that is of our interest, and in all iteration only this window size is considered.

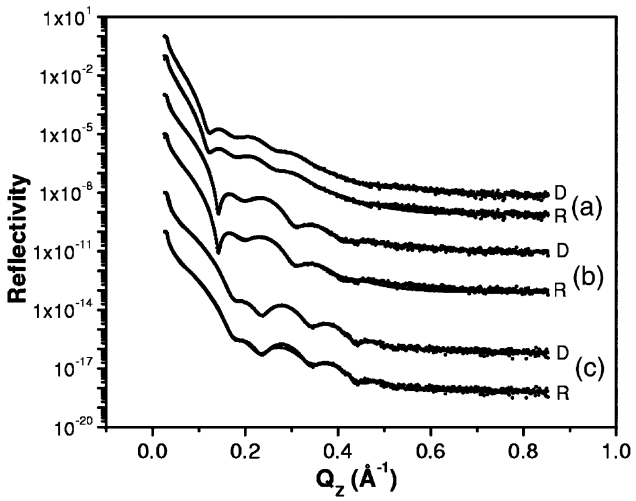

Fig. 1. Specular X-ray reflectivity data (●) for samples A, B and C, the solid lines marked D and R are the curves obtained from DWBA and recursive formalism, respectively.

3. Systems studied

3.1. Ultra-thin film of TiN

TiN thin films are commonly used as diffusion barrier and adhesion layer in integrated circuit devices [16]. Ultra-thin films of TiN have been deposited by metal-organic CVD from *tetrakis*-dimethylamino-titanium precursor on silicon wafers covered by native oxide. The deposition time was 10 s and a thickness of 100 Å is measured by ellipsometry. The as-deposited samples were then plasma-treated in N_2/H_2 atmosphere at RF = 750 W for 10, 20 and 40 s and labeled as sample A, B and C, respectively. Specular and off-specular X-ray reflectivity data were collected using laboratory X-ray source (Philips diffractometer) of wavelength 1.5419 Å. The off-specular intensity from all samples was found to be very small having values close to background count. The analysis schemes mentioned above are for 'true specular' reflectivity data. The 'true specular' reflectivity data are obtained by subtracting the off-specular contribution from the experimental specular reflectivity data or one has to add the background X-ray counts to the calculated reflectivity curve during analysis. In Fig. 1 we have shown the X-ray reflectivity data for the plasma-treated samples. The best reflectivity fit is shown as a solid line and is labeled as R for the fit obtained using three boxes by recursive method and labeled as D for the fit obtained by the DWBA formalism (*Note*: The number of boxes considered in the recursive method does not mean that the film consists

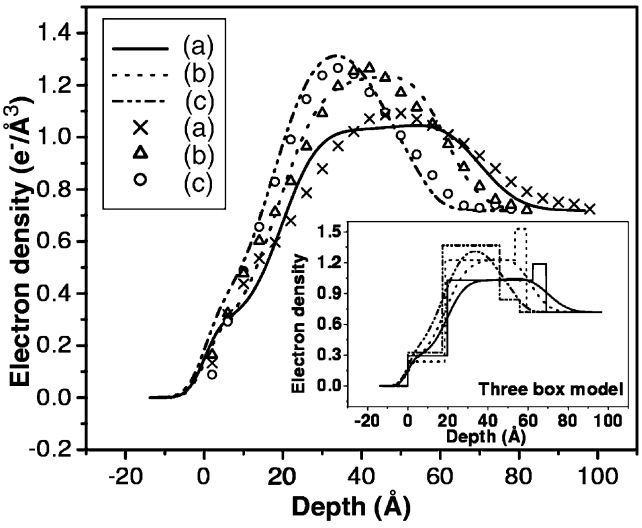

Fig. 2. EDP obtained from the DWBA (shown as symbols) and the recursive formalism (shown as lines) for samples A (cross), B (triangles) and C (circles). Inset: It shows the same EDP along with the electron density value as histograms to compare the EDP with the actual electron density values obtained from the recursive formalism for samples A (solid), B (dash) and C (dash dot dot).

of that many layers. It only provides a model to obtain the EDP of the film). In the inset of Fig. 2 we show the electron density values for each of the layers as histograms. The EDP is easily derived from the fit parameters. Since $d\rho/dz$ at each interface was considered to have a Gaussian form, the EDP $\rho(z)$ is represented by a series of error functions shown as smooth lines in the inset of Fig. 2. In the case of DWBA method, the thickness of each layer was fixed to 4 Å and 25, 21 and 20 numbers of layers were considered resulting to 96, 80 and 76 Å for sample A, B and C, respectively, as the total range of analysis. One generally takes in the DWBA scheme the range larger than the nominal total thickness of the film to make sure that some portion of the substrate is included in the analysis. The EDP that is obtained in this calculation does not depend on a priori model of the film and is therefore model-independent. The EDP obtained by this formalism is shown as symbols in Fig. 2. We observe from Fig. 2 that the EDP obtained from the recursive formalism and that from the DWBA formalism more or less fall on each other.

At a closer look in the inset of Fig. 2 one can see from the histograms that the samples A and B exhibit larger values of the electron density for the layer adjacent to the substrate. Convolution with an error functional form of interfacial roughness whose width is determined by the value of σ, and due to its larger value, results in lowering of the electron density. This is a direct consequence of a large value of σ obtained from the fit. We would like to stress here that the EDP obtained after the convolution is a more meaningful quantity than just the electron density value and its respective thickness for each of the layers. It is interesting to point out that σ values can be very large and its value can be close to that of layer thickness as was shown earlier [17]. This is so because in Eq. (1) k_n appears as a product with thickness d_n and the interfacial roughness σ_n and for fitting this cannot be separated out. Also, when one uses non-linear least square fitting technique to obtain the fit parameters, one generally obtains non-unique solutions and one has to choose from it the best fit parameters that appear more physical. Whereas, if one compares the EDP obtained from the recursive formalism with the parameters obtained from DWBA, one can to certain extent be more confident about the EDP even though we know one cannot be absolutely certain about the EDP obtained from the above two formalisms as we lose the phase information during the measurement of reflectivity. As mentioned in Section 2.2 that in DWBA one starts the fitting with $\Delta\rho_i = 0$ and for small variation in the electron density value from the average value of ρ_0, the fit parameters '$\Delta\rho_i$' converges to solution quickly as all the values are of the same order and one need not bother about the interfacial roughness to get the correct EDP in contrast to recursive formalism. From Fig. 2 we observe that the film thickness on plasma treatment reduces to $\sim$80, $\sim$70 and $\sim$60 Å for sample A, B and C, respectively. These values are obtained from the position of the depth where the value of the electron density approaches the value of the Si substrate. The air/film and film/substrate interfaces are not very sharp and the interface can be considered to be diffuse. We also observe that the electron density of the film increases with the plasma processing. The reduction of the film thickness as a function of plasma processing is due to the plasma etching. The carbon present in CVD film gives rise to complex polymeric structures of low density with embedded TiN clusters. The removal of carbon during plasma treatment causes TiN clusters to form a compact TiN film resulting in an increase in the electron density.

3.2. Ultra-thin oxynitride films

Dielectric films of oxynitride have replaced pure silicon oxide films as gate and tunnel oxide films in the ultra-large scale integrated technology because of its superior properties in terms of boron barrier, resistance to electrical stress and higher dielectric strength. The exact mechanism of the role of nitrogen in inhibiting boron diffusion is not completely clarified. The most interesting aspect is that the nitrogen places itself at the interface of SiO_2/Si independent of how it has been introduced by either NO or N_2O, and also independent on the condition of preparation. Characterization of nitrogen distribution in oxynitride thin films is becoming

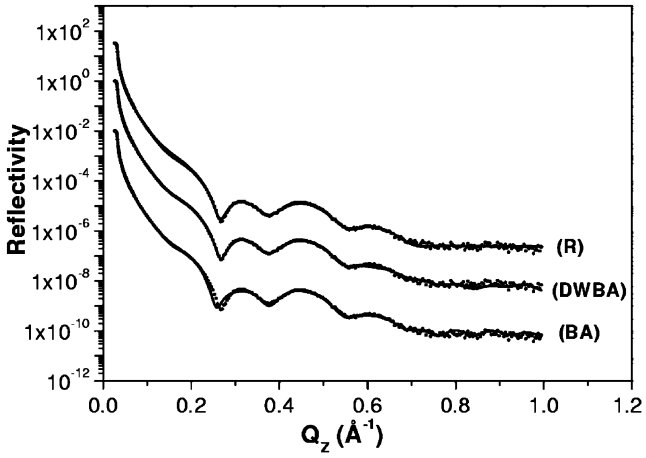

Fig. 3. Specular X-ray reflectivity data (●) of a SiO_2 film nitraded in NO atmosphere to form an oxynitride film, the solid lines are the fit obtained by recursive formalism (R), using DWBA formalism (DWBA) and Fourier inversion technique based on BA.

a very challenging task, given the extreme low thickness used in today's technology. The structural and chemical characterization of the oxynitride film has been carried out using the reflectivity technique. Here we would describe X-ray reflectivity analysis of an ultra-thin oxynitride film, grown from 3.5-nm wet oxides, by nitridation in NO atmosphere. Similarly, as in the above case the longitudinal specular and off-specular data were collected for GIXR measurement using laboratory X-ray source of wavelength 1.5419 Å, the off-specular intensity was found to be very small having the value close to background counts. Here we would like to compare the BA with DWBA and recursive formalism.

In Fig. 3 we show specular X-ray reflectivity for an ultra-thin oxynitride film. First we shall analyze the reflectivity data using the recursive formalism to obtain the EDP of the film as a function of depth. We assumed that the total film on the substrate consisted of mainly three layers, i.e. the top surface layer, the bulk oxide layer and a transition layer at the film/substrate interface. Using a three layer model we obtain the EDP from the recursive formalism as shown in Fig. 4. In Fig. 4 we have shown the EDP as a smooth solid line. We observe an increase of electron density in the transition layer at the interface of film/substrate. This increase of electron density at the interface of SiO_2/Si has been attributed to the accumulation of N as this was observed using secondary ion mass spectrometry analysis described in Ref. [18].

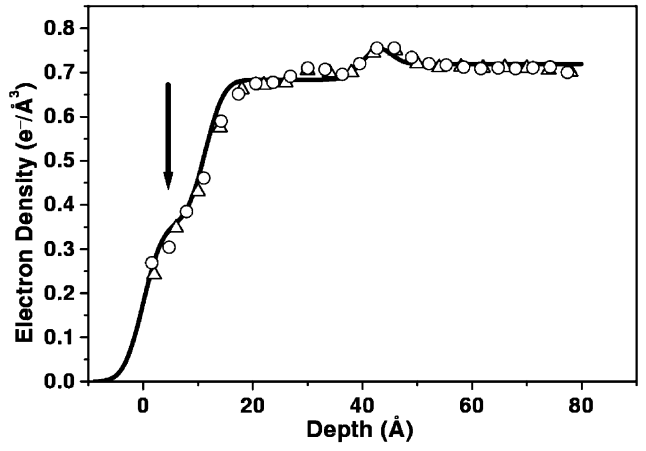

Fig. 4. EDP obtained using recursive formalism (solid line), DWBA (triangles) and BA (circles).

For the above sample we have also carried out the X-ray reflectivity analysis using a model-independent approach in the framework of DWBA and Fourier inverse technique based on BA. On the basis of the above two techniques, the reflectivity curves obtained are shown in Fig. 3. All of the three reflectivity curves obtained by the above three formalism fits the experimental data quite well. The EDP obtained from the above two formalisms are shown in Fig. 4 as symbols. Both formalisms give the same result, i.e. the EDP falls on each other. In Fig. 4 we have also compared the EDPs obtained from recursive formalism with that from DWBA and BA. The shoulder obtained from the recursive formalism at the surface of the film marked by an arrow was also obtained from the DWBA and BA formalisms. As mentioned earlier we can have better confidence about the EDP if all the above formalisms give similar EDP. Thus, we could say that one can reach a realistic solution for an ultra-thin film containing small variation in the EDP if one can compare the EDP with each of the above-mentioned methods.

4. Conclusion

We have shown that if an ultra-thin film consists of gradual variation in electron density as a function of depth, then one can fit the reflectivity profile using recursive formalism considering several layers and evaluating the EDP from the fit parameters. Since one can obtain various non-unique solutions that fit the reflectivity data, it becomes very important to obtain the EDP using the DWBA formalism and the BA. The DWBA formalism is based on non-linear least square fitting, whereas BA is based on an iterative method. By considering and comparing the EDP obtained from all the three methods, one can guess the structure of the system as a function of depth. We have also shown that to obtain gradual variation in the electron density as a function of depth we can introduce virtual layers. The thickness, electron density and the interfacial roughness individually may not have any significant meaning but the layers are just introduced to extract the right EDP as a function of depth, which is a more meaningful quantity.

Acknowledgments

We would like to acknowledge STMicroelectronics (Agrate, Milan, Italy) for providing TiN and oxynitride thin films.

References

[1] L.G. Parratt, Phys. Rev. 95 (1954) 359.
[2] M. Born, E. Wolf, Principles of Optics, sixth ed., Pergamon, London, 1980.
[3] B. Vidal, P. Vincent, Appl. Optics 23 (1984) 1794.
[4] A. Gibaud, in: J. Daillant, A. Giband (Eds.), X-ray and Neutron Reflectivity: Principles and Applications, Springer-Verlag, Berlin, 1999, p. 87.
[5] M.K. Sanyal, S.K. Sinha, A. Gibaud, K.G. Huang, B.L. Carvalho, M. Rafailovich, J. Sokolov, X. Zhao, W. Zhao, Europhys. Lett. 21 (1993) 691.
[6] X.-L. Zhou, S.H. Chen, Phys. Rep. 257 (1995) 233.
[7] S. Banerjee, M.K. Sanyal, A. Datta, S. Kanakaraju, S. Mohan, Phys. Rev. B 54 (1996) 16377.
[8] M.K. Sanyal, J.K. Basu, A. Datta, S. Banerjee, Europhys. Lett. 36 (1996) 265.
[9] S. Banerjee, S. Chakraborty, P.T. Lai, Appl. Phys. Lett. 80 (17) (2002) 3075.
[10] M. Li, M.O. Moller, G. Landwehr, J. Appl. Phys. 80 (5) (1996) 2788–2790.
[11] S. Banerjee, G. Raghavan, M.K. Sanyal, J. Appl. Phys. 85 (1999) 7135.
[12] N.W. Ashcroft, N.D. Mermin, Solid State Physics, Saunders College Publishing, 1976, p. 4.
[13] L. Nevot, P. Croce, Rev. Phys. Appl. 15 (1980) 761.
[14] J. Als-Neilsen, F. Christensen, P.S. Pershan, Phys. Rev. Lett. 48 (1982) 110.
[15] J. Als-Neilsen, Physica B+C 126 (1984) 145.
[16] M. Danek, M. Liao, J. Tseng, K. Littau, D. Saigal, H. Zhang, R. Mosely, M. Eizenberg, Appl. Phys. Lett. 68 (1996) 1015.
[17] S. Banerjee, A. Gibaud, D. Chateigner, S. Ferrari, C. Wiemer, D.T. Dekadjevi, Appl. Phys. Lett. 80 (3) (2002) 512.
[18] S. Banerjee, A. Gibaud, D. Chateigner, S. Ferrari, M. Fanciulli, J. Appl. Phys. 91 (1) (2002) 540.